AIMS Mathematics, 9(11): 31198–31216.
DOI: 10.3934/math.20241504
Received: 03 September 2024
Revised: 16 October 2024
Accepted: 18 October 2024
Published: 01 November 2024

https://www.aimspress.com/journal/Math

Research article

Multi-body dynamic evolution sequence-assisted PSO for interval analysis

Xuanlong Wu[1], Peng Zhong[1], Weihao Lin[1] and Jin Deng[2,*]

[1] State Key Laboratory of Structural Analysis, Optimization and CAE Software for Industrial Equipment, School of Mechanics and Aerospace Engineering, Dalian University of Technology, Dalian 116024, China
[2] Yunnan Branch of China Academy of Machinery Co., Ltd.

*** Correspondence:** Email: dengjin1989km@163.com.

Abstract: To enhance the efficiency and accuracy of response analysis in practical multivariable complex engineering problems, we introduced a new interval analysis method—multi-body dynamic evolution sequence-assisted particle swarm optimization (DES-PSO) is introduced in this research. This method optimizes the heterogeneous comprehensive learning particle swarm optimization algorithm (HCLPSO) by incorporating a dynamic evolution sequence (DES), addressing the difficulty of HCLPSO in covering the search space, which makes this method suitable for solving multivariable interval analysis problems. The results of two numerical examples prove that both DES-PSO and HCLPSO can give the accurate upper and lower bounds of the response interval. Compared with HCLPSO, DES-PSO improves the computing speed by about 50%.

Keywords: interval analysis; heterogeneous comprehensive learning particle swarm optimization algorithm; dynamic evolution; low discrepancy sequence
Mathematics Subject Classification: 68M15, 68T37

Abbreviations: PSO: particle swarm optimization; HCLPSO: heterogeneous comprehensive learning particle swarm optimization algorithm; DES: dynamic evolution sequence; DES-PSO: the method of improving HCLPSO with dynamic evolution sequence; LDS: low discrepancy sequence

1. Introduction

Uncertainty is pervasive in practical engineering problems, such as material properties [1–3], manufacturing errors [4–8], random loads [9–13], and service life [14,15]. The presence of uncertainty in measurement data and mathematical models is inevitable [16], and can significantly affect structural responses, necessitating evaluation. Coleman and Steele [17] pointed out that in an experiment where all measurements have only 1% uncertainty, the uncertainty of the experimental results can exceed 50%, implying that underestimating or incorrectly estimating uncertainty can severely impact the safety of engineering structures, potentially leading to catastrophic outcomes.

Therefore, it is crucial to consider the impact of uncertainty factors in structural analysis [18]. In practical engineering problems, due to limitations in experimental conditions and costs, some parameters cannot be accurately modeled with probability distributions due to insufficient experimental samples, leaving only their variation intervals available [19]. Given the interval uncertainty of input parameters, structural responses also exhibit interval uncertainty, making it vital to evaluate the interval uncertainty of responses. Failure to correctly estimate the variation range of responses could lead to erroneous judgments about the safety of materials or structures, posing serious safety risks [20]. Therefore, designing precise and efficient interval analysis methods for structural responses is of significant engineering importance.

Commonly used interval analysis methods include the Monte Carlo method (MCM), interval perturbation method, Chebyshev interval method, and vertex method. MCM provides stable solutions with sufficient sample data, which can ensure accuracy [21]. However, the computational costs will be greatly increased when facing large-scale engineering problems. Interval perturbation is a straightforward simplification method. Qiu et al. [22] solved displacement responses of uncertain parameters under small interval widths using the perturbation method, which later developed into the interval perturbation method [23]. However, the solution of this method may not converge under large interval dispersion. Xia et al. [24,25] proposed a sub-interval perturbation method to calculate the response domain of interval acoustic coupling systems. However, the computational burden grows significantly as the number of interval parameters and sub-intervals increases. Wu et al. [26,27] combined Chebyshev polynomial series expansion to address interval uncertainty, but the computational complexity of Chebyshev polynomial series increases exponentially with the number of parameters, leading to dimensionality issues. Qiu et al. [28,29] also combined finite element analysis with non-random convex models to propose the vertex method, suitable for solving exact boundaries of linear interval equations. However, this method is limited to monotonic cases, and its computational cost increases exponentially with interval parameters, making it impractical for large structural problems.

The essence of interval analysis lies in calculating the upper and lower bounds of structural responses based on the interval range of input parameters, which can be viewed as finding the maximum and minimum values of structural responses, thus forming two optimization problems.

Therefore, interval analysis problems can be solved by optimization algorithms. Common optimization problem-solving methods can be divided into two categories: Traditional gradient-based algorithms, characterized by fast convergence and high computational efficiency, but prone to getting trapped in local optima when dealing with multi-modal problems, and meta-heuristic intelligent optimization algorithms, which are less efficient than traditional gradient methods but have a strong ability to escape local optima and are considered effective for finding global optima. Many scholars have attempted to apply intelligent optimization algorithms to interval analysis. Feng et al. [30] applied the Bayesian global optimization algorithm to the interval estimation of safety factors in deterministic slope stability. Cheng et al. [31] proposed an improved Pelican algorithm and used it for interval analysis of free vibration responses of 3D pyramidal truss core sandwich panels. Ta et al. [32] proposed a new interval particle swarm optimization algorithm based on particle swarm optimization, applying it to interval analysis of vehicle body vibration and optimization of aerial camera stability.

From the above research, it is known that the result of interval analysis problems based on optimization algorithms is closely related to the computational performance of the optimization algorithms used. PSO is an excellent intelligent optimization algorithm based on meta-heuristic, which has a strong ability to jump out of local optimal and fast convergence speed [33], thus suitable for solving complex multivariable interval analysis problems. PSO has many excellent variants. Among them, HCLPSO [34] proposed by Lynn and Suganthan balances the global and local search capabilities of the PSO algorithm, which is recognized as one of the most outstanding variants of the famous PSO algorithm.

Wang et al. [35] present a novel saturated control method for a quadrotor to realize three–dimensional spatial trajectory tracking with HCLPSO. Yousri et al. [36] introduce a robust method to determine the permanent magnet synchronous motor model parameters efficiently and expeditiously based on HCLPSO. Wu et al. [37] introduce more shape parameters by HCLPSO, developing a novel multi-parameter wave spectrum model that substantially amplifies the capacity to describe the diversity of wave spectra. Yousri et al. [38] accurately extract the unknown parameters of a novel fractional order dynamic photovoltaic model by combining HCLPSO with chaos maps. Zhang et al. [39] solve large-scale optimization problems by introducing a random elite cognitive learning strategy and a stochastic dominant cognitive learning strategy into HCLPSO. Wang et al. [40] guarantee the convergence of the auxiliary sliding surfaces of the hierarchical sliding-mode control by optimizing the control parameters with HCLPSO. There have been many successful applications of HCLPSO, but there is no research on the application of this method to interval uncertainty analysis. HCLPSO has outstanding global and local search capabilities, which is expected to provide important help for constructing efficient and accurate interval analysis algorithms. However, HCLPSO optimizes by generating random sequences. It is difficult to effectively cover the search space due to the uneven distribution of point sets [41], which limits its computational efficiency in solving the high-dimensional complex interval uncertainty analysis problem.

In this paper, HCLPSO is first introduced to solve the interval uncertainty analysis problem. Because of the shortcoming that the original HCLPSO is difficult to effectively cover the search space, the multi-body dynamic evolution sequence (DES) [41] is used to optimize the distribution space and search direction of the particle swarm. The space coverage capability of HCLPSO is strengthened, forming a new interval uncertainty analysis method called DES-PSO. Compared with

the original method, the ability of DES-PSO to jump out of the local optimal is stronger, and the convergence speed is improved by about 50%. The calculation cost of the traditional interval analysis method often increases exponentially with the number of variables. DES-PSO, as an interval analysis method based on intelligent optimization algorithm, is of great significance in engineering and practice because of its lower computational cost and remarkable efficiency in dealing with multi-variable engineering problems.

The remainder of this paper is structured as follows: In Section 2, the interval problem is briefly introduced. In Section 3, we review the algorithmic principles of HCLPSO are reviewed. In Section 4, a new interval uncertainty analysis method DES-PSO is presented, which combines enhanced exploration and exploitation of heterogeneous particle swarm optimization with point sets generated by dynamic evolution algorithms. In Section 5, we validate the effectiveness of DES-PSO in handling interval uncertainty problems is validated through the solution of an interval equation system and an engineering case study involving the design of a smartwatch case. The conclusion is given in Section 6.

2. Brief introduction to interval problems

When dealing with practical engineering problems, it is often difficult to obtain a large amount of sample information, which makes it impossible to describe the uncertainty of random variables $\boldsymbol{X}$ with an exact probability distribution function. To address this issue, many scholars typically use the method of interval models to solve, which can greatly reduce time and computational costs. When characterizing its uncertainty using interval models, the uncertain variable $\boldsymbol{X}$ is referred to as an interval variable and can be represented as

$$\boldsymbol{X} = \left[x_1, x_2, \cdots, x_D\right], a_i \le x_i \le b_i, \tag{1}$$

where the subscript $i \in 1, 2, \cdots, D$, D denotes the number of variables, a_i and b_i represent the lower and upper bounds of the interval for the variable x_i, respectively.

Based on the interval variable $\boldsymbol{X}$, a general form of interval analysis model can be established as

$$\boldsymbol{Y} = \boldsymbol{f}\left(\boldsymbol{X}\right), \tag{2}$$

where $\boldsymbol{f}\left(\cdot\right)$ is the structural response function, and $\boldsymbol{Y}$ is the output uncertainty response.

Since $\boldsymbol{X}$ is interval variable, the output of the response function will vary within an interval rather than being a definite value, which is $\boldsymbol{Y} = \left[y_1, y_2, \cdots, y_M\right], y_i \in \left[y_{i,\min}, y_{i,\max}\right]$. Each y_i corresponds to a structural response function $f_i\left(\cdot\right)$. The purpose of interval uncertainty analysis is to determine the response interval of the response function, i.e., to ascertain the boundaries of the output response. Therefore, the problem of interval uncertainty analysis for a structure can be transformed into the following two optimization problems:

$$\begin{cases} y_{i,\min} = \min\left(f_i\left(\boldsymbol{X} \right) \right) \\ y_{i,\max} = \max\left(f_i\left(\boldsymbol{X} \right) \right) \end{cases}. \tag{3}$$

3. Brief introduction to HCLPSO

PSO is a population-driven evolutionary strategy [42]. In this strategy, each potential solution is symbolically represented as a soaring bird, which optimizes its position in the solution space based on its own flight experience and the experiences of other members of the population. Under the framework of HCLPSO [34], to achieve an in-depth exploration of the global search and fine exploitation of local search, the population is divided into two specialized subpopulations, each responsible for exploration and exploitation tasks.

To simplify our subsequent analysis process, HCLPSO is presented in a matrix-vector form, and the population size of the problem is defined as N, the maximum number of iterations as G, the objective function as f, and the feasible solution as $\boldsymbol{x} = \left(x_1, x_2, \cdots, x_D \right)^{\mathrm{T}} \in R^{D\times 1}$, where $x_i \in \left[a_i, b_i \right]$. Let

$$\boldsymbol{a} = \left(a_1, a_2, \cdots, a_D \right)^{\mathrm{T}}, \quad \boldsymbol{b} = \left(b_1, b_2, \cdots, b_D \right)^{\mathrm{T}}. \tag{4}$$

Let the population be represented as

$$\boldsymbol{X}_g = \left[\boldsymbol{x}_{g,1}, \boldsymbol{x}_{g,2}, \cdots, \boldsymbol{x}_{g,N} \right], \tag{5}$$

where the subscript g represents the g-th iteration step. The initial population in HCLPSO is

$$\boldsymbol{X}_0 = \boldsymbol{a} \otimes \boldsymbol{1}_N + \boldsymbol{\varepsilon}_0 \circ \left(\boldsymbol{b} \otimes \boldsymbol{1} - \boldsymbol{a} \otimes \boldsymbol{1} \right), \tag{6}$$

where $\otimes$ and $\circ$ denote the Kronecker product and the Hadamard product, respectively, $\boldsymbol{1}_N$ is a vector of size $1\times N$, with each element being 1, and $\boldsymbol{\varepsilon}_0$ is a matrix of random numbers uniformly distributed between 0 and 1, with a matrix size of $D\times N$.

When iterating the population of HCLPSO, the updating method is as follows:

$$\boldsymbol{x}_{g+1,i} = \boldsymbol{x}_{g,i} + \boldsymbol{v}_{g+1,i}, \quad i = 1, 2, \cdots, N, \tag{7}$$

where $\boldsymbol{v}_{g+1,i}$ is the velocity of the i-th particle. The population of HCLPSO is divided into exploration and exploitation subpopulations, with the sizes of the two types of subpopulations being N_1 and N_2, respectively, and their velocity updating formulas are also different. The expression for the velocity updating formula of the exploration subpopulation is

$$\boldsymbol{v}_{g+1,i} = w_g \boldsymbol{v}_{g,i} + k_g \boldsymbol{\varepsilon}_{g,1,i} \circ \left(\boldsymbol{p}_{g,i} - \boldsymbol{x}_{g,i} \right), \quad 1 \le i \le N_1, \tag{8}$$

where $w_g = 0.00 - 0.79g/G$ and $k_g = 3 - 0.5g/G$, $\boldsymbol{\varepsilon}_{g,1,i}$ is a vector of random numbers uniformly

distributed between 0 and 1, with a vector size of $D\times1$, and $\boldsymbol{p}_{g,i}$ is a random comprehensive learning vector, which enables the *i*-th particle to learn from the best experiences of all other particles. The relevant calculation formula for $\boldsymbol{p}_{g,i}$ can be found in Ref. [34]. The expression for the velocity updating formula of the exploitation subpopulation is

$$\boldsymbol{v}_{g+1,i} = w_g\boldsymbol{v}_{g,i} + c_{g,1}\boldsymbol{\varepsilon}_{g,2,i}\circ\left(\boldsymbol{p}_{g,i} - \boldsymbol{x}_{g,i}\right) + c_{g,2}\boldsymbol{\varepsilon}_{g,3,i}\circ\left(\boldsymbol{x}_{g,\text{best}} - \boldsymbol{x}_{g,i}\right),\ N_1 < i \le N, \tag{9}$$

where $c_{g,1} = 2.5 - 2g/G$ and $c_{g,2} = 0.5 + 2g/G$ are used in HCLPSO, $\boldsymbol{\varepsilon}_{g,2,i}$ and $\boldsymbol{\varepsilon}_{g,3,i}$ are two vectors of random numbers uniformly distributed between 0 and 1, with both vector sizes being $D\times1$, and $\boldsymbol{x}_{g,\text{best}} = \arg\min\left(f\left(\boldsymbol{x}_{g,i}\right)\right),\ 1\le i\le N$.

HCLPSO possesses outstanding global and local search capabilities, which are expected to provide significant assistance in constructing efficient and precise interval analysis algorithms. However, HCLPSO searches for optimization by generating random sequences, which has the drawback of potentially failing to effectively cover the search space due to the uneven distribution of the sequences.

4. The proposed method

In this section, an efficient interval analysis method is proposed to deal with multi-variable engineering problems. By introducing DES, this method improves the uniformity and coverage ability of the initial distribution of the particle swarm and expands the search range of the algorithm. Therefore, this method overcomes the shortcomings of HCLPSO in the search process due to the lack of sampling uniformity, and obtains a stronger ability to jump out of local optimal and faster convergence speed. In Section 4.1, the construction method of DES is briefly introduced. The DES-PSO obtained by improving HCLPSO based on DES is given in Section 4.2.

4.1. Dynamic evolution sequence

DES is a low discrepancy sequence (LDS) proposed in Refs. [41,43]. The concept of DES originates from an in-depth observation of physical phenomena, where many multi-body systems in nature have static solutions with good uniformity. In the DES, all particles in space are subject to gravitational forces acting between each other.

Assuming that all particles in space are within a hypercube $\boldsymbol{\Omega} = [0,1]^D$, where D denotes the spatial dimension, which is also the number of variables. The sample sequence is $\boldsymbol{X}_{D,N} = \left\{\boldsymbol{x}_1,\cdots x_i,\cdots,\boldsymbol{x}_N\right\}$, with each sample point considered as a star of mass m. The coordinates of the *i*-th star are $\boldsymbol{x}_i = \left(x_{i1},\cdots,x_{ik},\cdots x_{iD}\right)$, and there are interactive forces between points. The Lagrangian equations for these N stars are

$$\begin{cases} S = \int_0^t L \mathrm{d}\tau \\ L = \frac{1}{2} m \sum_{i=1}^{N} \sum_{k=1}^{D} \dot{x}_{ik}^2 - Q\left(\sum_{1 \le i < j \le N} \frac{1}{d_{q,ij}^p} \right)^{\frac{1}{p}}, \quad i, j, k, N, D \in N^*, \end{cases} \tag{10}$$

where $Q = 1$ is the generalized gravitational constant, $d_{q,ij}$ is the generalized distance between the i-th and j-th stars, q and p are control parameters that affect the optimization performance of the algorithm, with specific values available in Ref. [41], N^* denotes the set of positive integers. The expression for distance $d_{q,ij}$ is

$$d_{q,ij} = \sqrt{\sum_{k=1}^{D} \frac{\left| x_{ik} - x_{jk} \right|^2 \left(1 - \left| x_{ik} - x_{jk} \right| \right)^2}{\left[\left(1 - \left| x_{ik} - x_{jk} \right| \right)^q + \left| x_{ik} - x_{jk} \right|^q \right]^{\frac{2}{q}}}}. \tag{11}$$

According to the variational principle of Hamilton [44], it can be derived that

$$m\ddot{x}_{ik} + f_{ik} = 0, \ 1 \le i \le N, \ 1 \le k \le D, \tag{12}$$

where f_{ik} is the external force on the i-th star in the k-dimension. The expression of f_{ik} is

$$f_{ik} = -Q\left(\sum_{1 \le i < j \le N} \frac{1}{d_{q,ij}^p} \right)^{\frac{1-p}{p}} \sum_{\substack{j=1 \\ j \ne i}}^{N} \frac{a_{ijk}}{d_{q,ij}^{p+2}}, \tag{13}$$

where

$$a_{ijk} = \frac{\operatorname{sgn}\left(x_{ik} - x_{jk} \right) \Delta_{ijk} \left(1 - \Delta_{ijk} \right) \left[\left(1 - \Delta_{ijk} \right)^{q+1} - \Delta_{ijk}^{q+1} \right]}{\left[\left(1 - \Delta_{jik} \right)^q + \Delta_{ijk}^q \right]^{1+\frac{2}{q}}}, \quad \Delta_{ijk} = \left| x_{ik} - x_{jk} \right|. \tag{14}$$

For all sample points to reach a stationary state, an artificial damping force is applied to each sample, thus Eq (12) can be represented as the following common dynamical formula [45]:

$$m\ddot{x}_{ik} + c\dot{x}_{ik} + f_{ik} = 0, \ 1 \le i \le N, \ 1 \le k \le D, \tag{15}$$

where c is the damping coefficient.

Eqation (15) is a nonlinear dynamical equation. This subsection uses a symplectic algorithm [44,46] to discretize the equation: First, an initial sequence is given as $\boldsymbol{X}^{(0)} = \left\{ \boldsymbol{x}_1^{(0)}, \cdots, \boldsymbol{x}_N^{(0)} \right\}$, where $\boldsymbol{x}_{ik}^{(0)}$ represents the i-th sample point in the k-th dimension at the initial iteration step. The basic iteration formula of the algorithm can be expressed as

$$\begin{cases} x_{ik}^{(1)} = x_{ik}^{(0)} - \dfrac{1}{2} m^{-1} f_{ik}^{(0)} \Delta t^2 \\ x_{ik}^{(g+1)} = \dfrac{A_1 x_{ik}^{g} - A_2 x_{ik}^{(g-1)} - f_{ik}^{(g)}}{A_0} \end{cases}, \tag{16}$$

in which

$$\begin{cases} f_{ik}^{(g)} = -\left(\sum\limits_{1 \le i < j \le N} \dfrac{1}{\left(d_{q,ij}^{(g)} \right)^p} \right)^{\frac{1}{p}-1} \sum\limits_{\substack{j=1 \\ j \ne i}}^{N} \dfrac{a_{ijk}^{(g)}}{\left(d_{q,ij}^{(g)} \right)^{p+2}} \\ A_0 = \dfrac{m}{\Delta t^2} + \dfrac{c}{2\Delta t},\ A_1 = \dfrac{2m}{\Delta t^2},\ A_2 = \dfrac{m}{\Delta t^2} - \dfrac{c}{2\Delta t} \\ m = \dfrac{1+\kappa}{4} \dfrac{U\left(\boldsymbol{X}^{(0)} \right)}{\left\| \boldsymbol{X}^{(0)} \right\|_{\mathrm{F}}^2} \Delta t^2,\ \ c = \dfrac{U\left(\boldsymbol{X}^{(0)} \right)}{\left\| \boldsymbol{X}^{(0)} \right\|_{\mathrm{F}}^2} \sqrt{\kappa} \Delta t \end{cases}, \tag{17}$$

$\left\| \boldsymbol{X}^{(0)} \right\|_{\mathrm{F}}$ is the Frobenius norm, Δt and κ are also control parameters that affect the optimization performance of the algorithm, with specific values available in Ref. [41].

When all particles are in a stationary state, the generated sequence exhibits excellent uniformity, and this sequence has been proven to perform well in areas such as statistical problem-solving, intelligent optimization, experimental design, and physical model simulation [47–49].

4.2. Dynamic evolution sequence-assisted HCLPSO (DES-PSO)

From Eqs (6), (8), and (9), it can be seen that the initial population and velocity updating formulas of HCLPSO are random sequences, which have a relatively poor effect in covering the search space compared to uniformly distributed populations. In order to improve the search efficiency and solution quality of HCLPSO, the DES introduced in Subsection 4.1 is applied to HCLPSO in this subsection.

In this subsection, the random sequences in the velocity updating formulas of HCLPSO are replaced with the DES, and Eqs (8) and (9) are rewritten as

$$\boldsymbol{v}_{g+1,i} = w_g \boldsymbol{v}_{g,i} + k_g \boldsymbol{P}_i^{(1)} \circ \left(\boldsymbol{p}_{g,i} - \boldsymbol{x}_{g,i} \right),\ 1 \le i \le N_1, \tag{18}$$

$$\boldsymbol{v}_{g+1,i} = w_g \boldsymbol{v}_{g,i} + c_{g,1} \boldsymbol{P}_i^{(2)} \circ \left(\boldsymbol{p}_{g,i} - \boldsymbol{x}_{g,i} \right) + c_{g,2} \boldsymbol{\varepsilon}_{g,3,i} \circ \left(\boldsymbol{x}_{g,\mathrm{best}} - \boldsymbol{x}_{g,i} \right),\ N_1 < i \le N, \tag{19}$$

where $\boldsymbol{P}^{(1)} = \left(\boldsymbol{P}_1^{(1)}, \cdots, \boldsymbol{P}_{N_1}^{(1)} \right)$ is a DES of size $D \times N_1$, and $\boldsymbol{P}^{(2)} = \left(\boldsymbol{P}_1^{(2)}, \cdots, \boldsymbol{P}_{N-N_1}^{(2)} \right)$ is a DES of size $D \times \left(N - N_1 \right)$.

Similarly, the random initial population of HCLPSO is replaced with an initial population

generated by the DES, i.e.,

$$\boldsymbol{X}_0 = \boldsymbol{a} \otimes \boldsymbol{1}_N + \boldsymbol{P}^{(0)} \circ \left(\boldsymbol{b} \otimes \boldsymbol{1} - \boldsymbol{a} \otimes \boldsymbol{1} \right), \tag{20}$$

where $\boldsymbol{P}^{(0)}$ is a DES of size $D \times N$.

This paper names the method of improving HCLPSO with dynamic evolution sequence as DES-PSO. The DES-PSO pseudocode is shown in Table 1:

Table 1. The psseudocode of DES-PSO.

1.	Input D, $\boldsymbol{a}$, $\boldsymbol{b}$, N_1, N_2 and G; $N = N_1 + N_2$; $g = 0$;
2.	Initialize population $\boldsymbol{X}_0$ according to Eq (20);
3.	While $g < G$
4.	$g = g + 1$;
5.	Find $\boldsymbol{x}_{g,\text{best}} = \arg\min\left(f\left(x_{g,i} \right) \right),\ 1 \le i \le N$;
6.	For $i = 1 : N$
7.	If $1 \le i \le N_1$
8.	Update $\boldsymbol{v}_{g+1,i}$ according to Eq (18);
9.	Else
10.	Update $\boldsymbol{v}_{g+1,i}$ according to Eq (19);
11.	End
12.	$\boldsymbol{x}_{g+1,i} = \boldsymbol{x}_{g,i} + \boldsymbol{v}_{g+1,i}$;
13.	End
14.	End
15.	Find $\boldsymbol{x}_{G,\text{best}} = \arg\min\left(f\left(x_{G,i} \right) \right),\ 1 \le i \le N$;
16.	Output $\boldsymbol{x}_{G,\text{best}}$ as the solution.

By comparing Eqs (8) and (9) with Eqs (18) and (19), it can be seen that DES-PSO and HCLPSO have the same algorithm complexity. However, the result of each iteration of DES-PSO is better than that of HCLPSO because DES-PSO has a stronger ability to cover the search space. Therefore, the overall number of iteration steps required is lower and the efficiency is higher. Two numerical examples will be selected for comparison in the next section to verify the correctness and efficiency of DES-PSO.

5. Numerical examples

5.1. Linear interval equation systems

This example considers the solution of the following linear interval equation system, as shown in the following equation:

$$\begin{bmatrix} [3,6] & [-3,1.5] \\ [-1.5,3] & [3,6] \end{bmatrix} \begin{Bmatrix} x_1 \\ x_2 \end{Bmatrix} = \begin{Bmatrix} [-4,4] \\ [-4,4] \end{Bmatrix}. \tag{21}$$

This problem was studied in Ref. [50] and the solution domain was plotted, as shown in Figure 1. From Figure 1, it can be seen that the solution domain of this problem is non-convex, and the optimization problem at this time may have more than one extreme point. This requires the use of a stochastic optimization algorithm for solving.

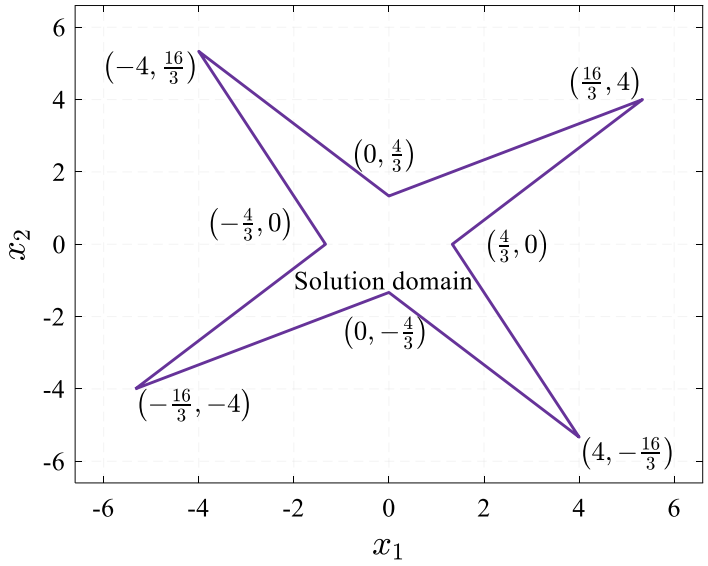

Figure 1. The solution domain of Eq (21). The region enclosed by the four-pointed star is the possible distribution region of all the solutions (x_1, x_2) of the Eq (21).

In this subsection, the DES-PSO proposed in Subsection 4.2 and the original HCLPSO algorithm are used to solve this interval equation system simultaneously. The computational results show that both algorithms can obtain the exact upper and lower bounds, namely $[x_1] = [-16/3, 16/3]$ and $[x_2] = [-16/3, 16/3]$. This proves that both the DES-PSO and the original HCLPSO algorithms have good optimization accuracy. To further compare the computational efficiency of the two algorithms, the number of convergence steps required for each algorithm to find the exact solution of the interval upper and lower bounds is counted, and the results are listed in Table 2.

Table 2. Comparison of convergence steps of two algorithms.

Variable name	Interval lower bound		Interval upper bound	
	DES-PSO	HCLPSO	DES-PSO	HCLPSO
x_1	2452	3371	2249	3211
x_2	1904	3779	1379	3077

From Table 2, it can be seen that the convergence speed of DES-PSO is much faster than the convergence speed of the original HCLPSO. To better measure the degree of speed improvement, we introduce the relative speedup percentage as a measure of acceleration. The relative percentage can be expressed as (HCLPSO convergence steps - DES-PSO convergence steps)/DES-PSO convergence steps $\times 100\%$. When solving the lower bound of x_1, DES-PSO can achieve a relative speedup of 27.26%, and when solving the upper bound of x_1, DES-PSO can achieve a relative speedup of 30.93%. When solving the lower bound of x_2, DES-PSO can achieve a relative speedup of 49.61%, and when solving the upper bound of x_2, DES-PSO can achieve a relative speedup of 55.18%. Combining the results from Table 2, it can be concluded that our improved algorithm is more computationally efficient when dealing with interval problems.

5.2. Uncertainty interval analysis of smartwatches

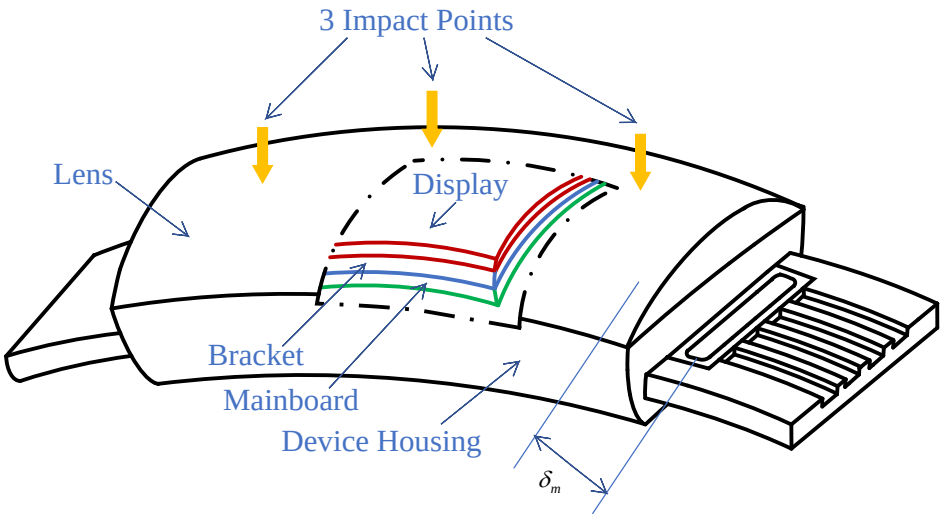

Figure 2. Schematic diagram of the smart watch.

Dynamic impact analysis [51–53] and heat conduction analysis [54–56] play significant roles in the field of engineering applications, especially for precision electronic devices [57]. Wearable electronic devices have a high degree of integration, during the design process, it is necessary to consider the requirements of mechanical, electrical, and thermal performance simultaneously. For example, it is necessary to ensure that the stress and the temperature of the embedded chips in the watch are within a reliable working range under impact conditions and high-temperature environments. This example uses the smartwatch model provided in Ref. [58], which is shown in Figure 2. This example studies the stress σ_1^N, σ_2^N, and σ_3^N distribution intervals of the three different impact points shown in Figure 2, under impact conditions, and the stress σ^H of the solder between the display and the mainboard, as well as the temperature T_1 and T_2 distribution intervals of the two embedded chips in the smartwatch under high-temperature environments.

The random variables and their distribution intervals in the watch are shown in Table 3. The interval random variables such as the smartwatch shell thickness, mainboard thickness, bracket thickness, and display thickness have a significant impact on the stress at the impact points and the chip temperature. Therefore, 65 finite element samples are used in [58], considering the 10 interval

random variables in Table 3, to construct the response surface functions for the stress and temperature of the smartwatch, as detailed in Table 4.

Table 3. Interval parameters of random variables.

Variable name	Random variable	Distribution interval
Shell thickness	$X_1(\text{mm})$	$(0.91,1.09)$
Mainboard thickness	$X_2(\text{mm})$	$(0.91,1.09)$
Bracket thickness	$X_3(\text{mm})$	$(0.91,1.09)$
Display thickness	$X_4(\text{mm})$	$(0.91,1.09)$
Lens thickness	$X_5(\text{mm})$	$(0.91,1.09)$
Young modulus of mainboard	$P_1(\text{MPa})$	$(10400,11600)$
Young modulus of Display	$P_2(\text{MPa})$	$(22600,23400)$
Young modulus of Lens	$P_3(\text{MPa})$	$(2380,2580)$
Power consumption of chip 1	$P_4(\text{W})$	$(0.09,0.21)$
Power consumption of chip 2	$P_5(\text{W})$	$(0.09,0.21)$

Table 4. Six response surface functions.

Variable	Response surface function
$\sigma_1^N(\text{MPa})$	$\sigma_1^N=(0.001848P_2^2-0.3688P_2P_3+973.18P_2+1.609P_3^2)\times10^{-6}-30.19X_1^2$ $+1.133X_1X_3+33.10X_1X_4+1.313X_1X_5+0.4128X_3^2-3.7317X_3X_4$ $-0.26871X_3X_5-56.55X_4^2+65.54X_4X_5-55.32X_5^2+129.86$
$\sigma_2^N(\text{MPa})$	$\sigma_2^N=(-0.03509P_2^2+0.1813P_2P_3+1277P_2-1.461P_3^2)\times10^{-6}-35.80X_1^2$ $+6.112X_1X_3+32.86X_1X_4+2.891X_1X_5-6.809X_3^2+4.303X_3X_4$ $+9.209X_3X_5-63.71X_4^2+67.43X_4X_5-64.37X_5^2+135.2$
$\sigma_3^N(\text{MPa})$	$\sigma_3^N=(0.03054P_2^2-0.95P_2P_3+802.6P_2+4.645P_3^2)\times10^{-6}-28.19X_1^2$ $+4.188X_1X_3+28.63X_1X_4+0.2030X_1X_5+9.152X_3^2-16.12X_3X_4$ $-15.75X_3X_5-42.17X_4^2+62.61X_4X_5-36.32X_5^2+119.5$
$\sigma^H(\text{MPa})$	$\sigma^H=0.0000002578P_1^2-0.00002501P_1X_2-0.9103X_1^2+0.02502X_1X_2$ $+0.6950X_1X_3+0.1007X_2^2+0.0125X_2X_3-2.372X_3^2+37.54$
$T_1(^\circ\text{C})$	$T_1=0.5473X_1^2-2.932X_1X_2-0.3207X_1X_3+5.589X_2^2$ $-2.970X_2X_3-1.206X_3^2+71.85P_4+72.81P_5+299.3P_4P_5+62.05$
$T_2(^\circ\text{C})$	$T_2=0.5448X_1^2-2.923X_1X_2-0.3219X_1X_3+5.569X_2^2$ $-2.973X_2X_3-1.204X_3^2+61.10P_4+96.78P_5+255.2P_4P_5+61.11$

The DES-PSO proposed in Subsection 4.2 and the original HCLPSO are used to simultaneously optimize the six response surface functions listed in Table 4, with the computational results presented in Table 5. It can be seen from Table 5 that both algorithms can obtain the exact upper and lower bounds for the six surrogate models, indicating that both the improved HCLPSO algorithm and the original HCLPSO algorithm have good optimization accuracy. To further compare the computational efficiency of the two algorithms, the number of convergence steps required for each algorithm to find

the exact solutions for the interval upper and lower bounds is counted and listed in Table 6.

Table 5. Comparison of the results of two algorithms.

Variable	Lower bound of the interval		Upper bound of the interval	
	DES-PSO	HCLPSO	DES-PSO	HCLPSO
$\sigma_1^N\left(\mathrm{MPa}\right)$	89.060	89.060	105.318	105.318
$\sigma_2^N\left(\mathrm{MPa}\right)$	66.908	66.908	89.221	89.221
$\sigma_3^N\left(\mathrm{MPa}\right)$	26.612	26.612	47.865	47.865
$\sigma^H\left(\mathrm{MPa}\right)$	62.230	62.230	69.937	69.937
$T_1\left(^{\mathrm{o}}\mathrm{C}\right)$	75.104	75.104	105.603	105.603
$T_2\left(^{\mathrm{o}}\mathrm{C}\right)$	74.984	74.984	105.475	105.475

From Table 6, it can be seen that DES-PSO has a significantly faster convergence rate than the original HCLPSO algorithm. In the process of determining the lower bounds of the six response surface functions, the convergence speed of DES-PSO is on average 57.96% faster than the original algorithm, with the highest improvement being 62.80%. In the process of determining the upper bounds of the six response surface functions, the convergence speed of the improved algorithm is on average 56.71% faster than the original algorithm, with the maximum improvement being 60.56%. These results indicate that DES-PSO can efficiently handle multivariable uncertainty interval analysis problems.

Table 6. Comparison of convergence steps of two algorithms.

Variable	Lower bound of the interval		Upper bound of the interval	
	DES-PSO	HCLPSO	DES-PSO	HCLPSO
σ_1^N	958	2287	985	2249
σ_2^N	1114	2499	1070	2436
σ_3^N	1061	2415	1105	2480
σ^H	667	1793	773	1960
T_1	922	2224	1000	2313
T_2	998	2314	1095	2446
Average improvement	57.96%		56.71%	

6. Conclusions

In order to construct an accurate and efficient method for interval uncertainty analysis, HCLPSO is introduced into interval analysis in this paper. Aiming at the issue of high computational cost in traditional HCLPSO, we optimize the random search mechanism of HCLPSO is optimized with the DES, constructing a new efficient interval analysis method, DES-PSO. The newly proposed method is applied to the solution of interval equation systems and the design of smartwatch casings. It is proved that the newly proposed DES-PSO can significantly improve computational efficiency while ensuring calculation accuracy, thus having a good ability to solve multi-variable engineering problems.

The study, while valuable, has certain limitations. Although DES can be constructed in advance, the computational costs for the first time to construct DES with dimensions higher than 20 or particle

numbers greater than 1000 can not be negligible. Meanwhile, it needs to rely on experience to determine the number of particles needed to solve the problem when solving specific problems. When the number of particles is insufficient, there is a risk that the optimal solution will not be found. When the number of particles is too large, the calculation time is large. In addition, we use only the DES-PSO algorithm is only used to solve the interval model problem in this paper. In future research, we aim to employ DES-PSO to interval processes and interval field problems [59,60].

Author contributions

Xuanlong Wu: methodology, software, validation, writing–original draft, writing–review & editing; Peng Zhong: conceptualization, methodology, project administration, supervision, funding acquisition, writing–review & editing; Weihao Lin: methodology, writing–review & editing, resources; Jin Deng: methodology, software, investigation. All authors have read and approved the final version of the manuscript for publication.

Acknowledgments

This work was supported by the “National Key R&D Program” regional multi-mode collaboration and innovative industrial software platform (No. 2023YFB3308800).

Conflict of interest

We declare that we have no financial or personal relationships with other people or organizations that can inappropriately influence our work. There is no professional or other personal interest of any nature or kind in any product, service and/or company that could be construed as influencing the position presented in, or the review of, the manuscript entitled.

References

1. F. Wu, D. W. Huang, X. M. Xu, K. Zhao, N. Zhou, An adaptive divided-difference perturbation method for solving stochastic problems, *Struct. Saf.*, **103** (2023), 102346. https://doi.org/10.1016/j.strusafe.2023.102346
2. F. Wu, Q. Gao, X. M. Xu, W. X. Zhong, Expectation-based approach for one-dimensional randomly disordered phononic crystals, *Phys. Lett. A*, **378** (2014), 1043–1048. https://doi.org/10.1016/j.physleta.2014.02.031
3. H. B. Motra, J. Hildebrand, F. Wuttke, The Monte Carlo Method for evaluating measurement uncertainty: Application for determining the properties of materials, *Probabilisti. Eng. Mech.*, **45** (2016), 220–228. https://doi.org/10.1016/j.probengmech.2016.04.005
4. F. Wu, W. X. Zhong, *A hybrid approach for the time domain analysis of linear stochastic structures, Comput. Method. Appl. M.*, **265** (2013), 71–82. https://doi.org/10.1016/j.cma.2013.06.006

5. F. Wu, Q. Gao, X. M. Xu, W. X. Zhong, A modified computational scheme for the stochastic perturbation finite element method, *Lat. Am. J. Solids Struct.*, **12** (2015), 2480–2505. https://doi.org/10.1590/1679-78251772
6. D. W. Huang, F. Wu, S. Zhang, B. S. Chen, H. W. Zhang, A high-performance calculation scheme for stochastic dynamic problems, *Mech. Syst. Signal Pr.*, **189** (2023), 110073. https://doi.org/10.1016/j.ymssp.2022.110073
7. D. W. Huang, F. Wu, C. Z. Li, H. W. Zhang, The application of adaptive divided-difference perturbation method for stochastic problems with multimodal distribution, *3rd International Conference on Applied Mathematics, Modelling and Intelligent Computing (CAMMIC 2023)*, Tangshan, China, 2023, 1275617. https://doi.org/10.1117/12.2685895
8. Y. L. Zong, N. G. Hu, B. Y. Duan, G. G. Yang, H. J. Cao, W. Y. Xu, Manufacturing error sensitivity analysis and optimal design method of cable-network antenna structures, *Acta Astronaut.*, **120** (2016), 182–191. https://doi.org/10.1016/j.actaastro.2015.11.026
9. F. Wu, K. Zhao, L. L. Zhao, C. Y. Chen, W. X. Zhong, Uncertainty analysis of the control rod drop based on the adaptive collocation stochastic perturbation method, *Ann. Nucl. Energy*, **190** (2023), 109873. https://doi.org/10.1016/j.anucene.2023.109873
10. Y. X. Yang, K. Zhao, Y. L. Zhao, F. Wu, C. Y. Chen, J. Yan, et al., UA-CRD, a computational framework for uncertainty analysis of control rod drop with time-variant epistemic uncertain parameters, *Ann. Nucl. Energy*, **195** (2024), 110171. https://doi.org/10.1016/j.anucene.2023.110171
11. M. Salari, Fatigue crack growth reliability analysis under random loading, *Int. J. Struct. Integr.*, **11** (2020), 157–168. https://doi.org/10.1108/IJSI-06-2019-0053
12. D. W. Huang, F. Wu, Y. L. Zhao, J. Yan, H. W. Zhang, Application of high-credible statistical results calculation scheme based on least squares Quasi-Monte Carlo method in multimodal stochastic problems, *Comput. Method. Appl. M.*, **418** (2024), 116576. https://doi.org/10.1016/j.cma.2023.116576
13. L. Zhu, K. Q. Ye, D. W. Huang, F. Wu, W. X. Zhong, An adaptively filtered precise integration method considering perturbation for stochastic dynamics problems, *Acta Mech. Solida Sin.*, **36** (2023), 317–326. https://doi.org/10.1007/s10338-023-00381-4
14. Y. F. Ma, Z. Z. Guo, L. Wang, J. R. Zhang, Probabilistic life prediction for reinforced concrete structures subjected to seasonal corrosion-fatigue damage, *J. Struct. Eng.*, **146** (2020), 7. https://doi.org/10.1061/(ASCE)ST.1943-541X.0002666
15. H. J. Peng, F. J. Sun, F. Wu, D. X. Yang, Dynamic reliability of mechanism based on direct probability integral method, *Int. J. Mech. Sci.*, **270** (2024), 109105. https://doi.org/10.1016/j.ijmecsci.2024.109105
16. Y. B. Chen, M. L. Wen, Q. Y. Zhang, Y. Zhou, R. Kang, Generalized first-order second-moment method for uncertain random structures, *AIMS Mathematics*, **8** (2023), 13454–13472. https://doi.org/10.3934/math.2023682
17. H. W. Coleman, W. G. Steele, *Experimentation, validation, and uncertainty analysis for engineers*, Hoboken: John Wiley & Sons, 2018. https://doi.org/10.1002/9781119417989

18. Y. Z. Wang, Y. F. Zong, J. L. McCreight, J. D. Hughes, A. M. Tartakovsky, Bayesian reduced-order deep learning surrogate model for dynamic systems described by partial differential equations, *Comput. Method. Appl. M.*, **429** (2024), 117147. https://doi.org/10.1016/j.cma.2024.117147
19. D. M. Do, W. Gao, C. M. Song, M. Beer, Interval spectral stochastic finite element analysis of structures with aggregation of random field and bounded parameters, *Int. J. Numer. Meth. Eng.*, **108** (2016), 1198–1229. https://doi.org/10.1002/nme.5251
20. C. Hao, J. Ma, N. Xu, Q. Zhao, J. Y. Du, K. J. Zhu, Uncertainty propagation analysis for control rod worth of PWR based on the statistical sampling method, *Ann. Nucl. Energy*, **137** (2020), 107054. https://doi.org/10.1016/j.anucene.2019.107054
21. H. Zhang, H. Z. Dai, M. Beer, W. Wang, Structural reliability analysis on the basis of small samples: An interval quasi-Monte Carlo method, *Mech. Syst. Signal Pr.*, **37** (2013), 137–151. https://doi.org/10.1016/j.ymssp.2012.03.001
22. Z. P. Qiu, S. H. Chen, D. T. Song, The displacement bound estimation for structures with an interval description of uncertain parameters, *Commun. Numer. Meth. En.*, **12** (1996), 1–11. https://doi.org/10.1002/(sici)1099-0887(199601)12:1<1::aid-cnm884>3.0.co;2-n
23. Z. P. Qiu, I. Elishakoff, Antioptimization of structures with large uncertain-but-non-random parameters via interval analysis, *Comput. Method. Appl. M.*, **152** (1998), 361–372. https://doi.org/10.1016/S0045-7825(96)01211-X
24. B. Z. Xia, D. J. Yu, J. Liu, Interval and subinterval perturbation methods for a structural-acoustic system with interval parameters, *J. Fluid. Struct.*, **38** (2013), 146–163. https://doi.org/10.1016/j.jfluidstructs.2012.12.003
25. B. Z. Xia, D. J. Yu, Modified interval and subinterval perturbation methods for the static response analysis of structures with interval parameters, *J. Struct. Eng.*, **140** (2014), 04013113. https://doi.org/10.1061/(ASCE)ST.1943-541X.0000936
26. J. L. Wu, Y. Q. Zhang, L. P. Chen, Z. Luo, A Chebyshev interval method for nonlinear dynamic systems under uncertainty, *Appl. Math. Model.*, **37** (2013), 4578–4591. https://doi.org/10.1016/j.apm.2012.09.073
27. J. L. Wu, Z. Luo, Y. Q. Zhang, N. Zhang, L. P. Chen, Interval uncertain method for multibody mechanical systems using Chebyshev inclusion functions, *Int. J. Numer. Meth. Eng.*, **95** (2013), 608–630. https://doi.org/10.1002/nme.4525
28. Z. P. Qiu, Comparison of static response of structures using convex models and interval analysis method, *Int. J. Numer. Meth. Eng.*, **56** (2003), 1735–1753. https://doi.org/10.1002/nme.636
29. Z. P. Qiu, Y. Y. Xia, J. L. Yang, The static displacement and the stress analysis of structures with bounded uncertainties using the vertex solution theorem, *Comput. Method. Appl. M.*, **196** (2007), 4965–4984. https://doi.org/10.1016/j.cma.2007.06.022
30. C. X. Feng, M. Faes, M. Broggi, C. Dang, J. S. Yang, Z. B. Zheng, et al., Application of interval field method to the stability analysis of slopes in presence of uncertainties, *Comput. Geotech.*, **153** (2023), 105060. https://doi.org/10.1016/j.compgeo.2022.105060

31. Y. G. Chen, R. Zhong, Q. S. Wang, L. M. Chen, B. Qin, Free vibration analysis and multi-objective robust optimization of three-dimensional pyramidal truss core sandwich plates with interval uncertain parameters, *Eur. J. Mech. A-Solid.*, **108** (2024), 105401. https://doi.org/10.1016/j.euromechsol.2024.105401
32. N. Ta, Z. W. Zheng, H. C. Xie, An interval particle swarm optimization method for interval nonlinear uncertain optimization problems, *Adv. Mech. Eng.*, **15** (2023), 1–14. https://doi.org/10.1177/16878132231153266
33. K. Bhatt, H. Kumar, A new hybrid particle swarm optimization algorithm for optimal tasks scheduling in distributed computing system, *Intelligent Systems with Applications*, **18** (2023), 200219. https://doi.org/10.1016/j.iswa.2023.200219
34. N. Lynn, P. N. Suganthan, Heterogeneous comprehensive learning particle swarm optimization with enhanced exploration and exploitation, *Swarm Evol. Comput.*, **24** (2015), 11–24. https://doi.org/10.1016/j.swevo.2015.05.002
35. J. J. Wang, G. Y. Liu, Saturated control design of a quadrotor with heterogeneous comprehensive learning particle swarm optimization, *Swarm Evol. Comput.*, **46** (2019), 84–96. https://doi.org/10.1016/j.swevo.2019.02.008
36. D. Yousri, D. Allam, M. B. Eteiba, P. N. Suganthan, Chaotic heterogeneous comprehensive learning particle swarm optimizer variants for permanent magnet synchronous motor models parameters estimation, *Iran. J. Sci. Technol. Trans. Electr. Eng.*, **44** (2020), 1299–1318. https://doi.org/10.1007/s40998-019-00294-4
37. F. Wu, L. Zhu, Y. L. Zhao, C. F. Ai, X. Wang, F. Cai, et al., Wave spectrum fitting with multiple parameters based on optimization algorithms and its application, *Ocean Eng.*, **312** (2024), 119073. https://doi.org/10.1016/j.oceaneng.2024.119073
38. D. Yousri, D. Allam, M. B. Eteiba, P. N. Suganthan, Static and dynamic photovoltaic models' parameters identification using chaotic heterogeneous comprehensive learning particle swarm optimizer variants, *Energy Convers. Manage.*, **182** (2019), 546–563. https://doi.org/10.1016/j.enconman.2018.12.022
39. E. Zhang, Z. H. Nie, Q. Yang, Y. Q. Wang, D. Liu, S. W. Jeon, et al., Heterogeneous cognitive learning particle swarm optimization for large-scale optimization problems, *Inform. Sciences*, **633** (2023), 321–342. https://doi.org/10.1016/j.ins.2023.03.086
40. J. J. Wang, G. Y. Liu, Hierarchical sliding-mode control of spatial inverted pendulum with heterogeneous comprehensive learning particle swarm optimization, *Inform. Sciences*, **495** (2019), 14–36. https://doi.org/10.1016/j.ins.2019.05.004
41. F. Wu, Y. L. Zhao, K. Zhao, W. X. Zhong, A multi-body dynamical evolution model for generating the point set with best uniformity, *Swarm Evol. Comput.*, **73** (2022), 101121. https://doi.org/10.1016/j.swevo.2022.101121
42. Y. Sun, Y. L. Gao, An improved composite particle swarm optimization algorithm for solving constrained optimization problems and its engineering applications, *AIMS Mathematics*, **9** (2024), 7917–7944. https://doi.org/10.3934/math.2024385
43. Y. L. Zhao, F. Wu, Y. X. Yang, X. D. Wei, Z. H. Hu, J. Yan, et al., Constructing uniform design tables based on restart discrete dynamical evolutionary algorithm, *Soft Comput.*, **28** (2024), 11515–11534. https://doi.org/10.1007/s00500-024-09890-x

44. F. Wu, W. X. Zhong, Constrained Hamilton variational principle for shallow water problems and Zu-class symplectic algorithm, *Appl. Math. Mech.*, **37** (2016), 1–14. https://doi.org/10.1007/s10483-016-2051-9
45. F. Wu, L. Zhu, Y. L. Zhao, K. L. Zhang, J. Yan, W. X. Zhong, et al., Efficient computational method for matrix function in dynamic problems, *Acta Mech. Sin.*, **39** (2023), 522451. https://doi.org/10.1007/s10409-023-22451-x
46. K. Zhao, X. M. Xu, C. Y. Chen, F. Wu, D. W. Huang, Y. Y. Xi, et al., Nonlinear state equation and adaptive symplectic algorithm for the control rod drop, *Ann. Nucl. Energy*, **179** (2022), 109402. https://doi.org/10.1016/j.anucene.2022.109402
47. F. Wu, Y. L. Zhao, Y. X. Yang, X. P. Zhang, N. Zhou, A new discrepancy for sample generation in stochastic response analyses of aerospace problems with uncertain parameters, *Chinese J. Aeronaut.*, in press. https://doi.org/10.1016/j.cja.2024.09.044
48. Y. L. Zhao, F. Wu, J. H. Pang, W. X. Zhong, Updating velocities in heterogeneous comprehensive learning particle swarm optimization with low-discrepancy sequences, 2022, arXiv: 2209.09438. https://doi.org/10.48550/arXiv.2209.09438
49. F. Wu, Y. L. Zhao, J. H. Pang, J. Yan, W. X. Zhong, Low-discrepancy sampling in the expanded dimensional space: An acceleration technique for particle swarm optimization, 2023, arXiv: 2303.03055. https://doi.org/10.48550/arXiv.2303.03055
50. D. G. Wang, J. Li, A reliable approach to compute the static response of uncertain structural system, *Chinese Journal of Computational Mechanics*, **20** (2003), 662–669. https://doi.org/10.3969/j.issn.1007-4708.2003.06.004
51. F. Wu, K. Zhao, X. L. Wu, H. J. Peng, L. L. Zhao, W. X. Zhong, A time-averaged method to analyze slender rods moving in tubes, *Int. J. Mech. Sci.*, **279** (2024), 109510. https://doi.org/10.1016/j.ijmecsci.2024.109510
52. J. Zhang, Q. Gao, F. Wu, W. X. Zhong, A linear complementarity method for the solution of vertical vehicle–track interaction, *Vehicle Syst. Dyn.*, **56** (2018), 281–296. https://doi.org/10.1080/00423114.2017.1372585
53. S. Campbell, B. Vacchini, Collision models in open system dynamics: A versatile tool for deeper insights, *Europhysics Letters*, **133** (2021), 60001. https://doi.org/10.1209/0295-5075/133/60001
54. D. W. Huang, Y. L. Zhao, K. Q. Ye, F. Wu, H. W. Zhang, W. X. Zhong, The efficient calculation methods for stochastic nonlinear transient heat conduction problems, *J. Comput. Sci.*, **67** (2023), 101939. https://doi.org/10.1016/j.jocs.2022.101939
55. F. Wu, W. X. Zhong, A modified stochastic perturbation method for stochastic hyperbolic heat conduction problems, *Comput. Method. Appl. M.*, **305** (2016), 739–758. https://doi.org/10.1016/j.cma.2016.03.032
56. F. Wu, Q. Gao, W. X. Zhong, Fast precise integration method for hyperbolic heat conduction problems, *Appl. Math. Mech.*, **34** (2013), 791–800. https://doi.org/10.1007/s10483-013-1707-6
57. X. L. Zhang, Z. Ji, J. F. Wang, X. Lv, Research progress on structural optimization design of microchannel heat sinks applied to electronic devices, *Appl. Therm. Eng.*, **235** (2023), 121294. https://doi.org/10.1016/j.applthermaleng.2023.121294

58. Z. L. Huang, C. Jiang, Y. S. Zhou, Z. Luo, Z. Zhang, An incremental shifting vector approach for reliability-based design optimization, *Struct. Multidisc. Optim.*, **53** (2016), 523–543. https://doi.org/10.1007/s00158-015-1352-7
59. B. Y. Ni, C. Jiang, Interval field model and interval finite element analysis, *Comput. Method. Appl. M.*, **360** (2020), 112713. https://doi.org/10.1016/j.cma.2019.112713
60. B. Y. Ni, C. Jiang, J. W. Li, W. Y. Tian, Interval K-L expansion of interval process model for dynamic uncertainty analysis, *J. Sound Vib.*, **474** (2020), 115254. https://doi.org/10.1016/j.jsv.2020.115254

AIMS Press